

Early Phases and Initial Conditions for Massive Star Formation

Neal J. Evans II, Yancy L. Shirley, Kaisa E. Mueller, & Claudia Knez
*Department of Astronomy, The University of Texas at Austin, Austin,
Texas 78712-1083*

Abstract. Our knowledge of the initial conditions and early stages of high mass star formation is very limited. We will review recent surveys of regions in the early stages of massive star formation using molecular tracers of high density and dust continuum emission and consider the status of evolutionary schemes. Comparison to the situation for low mass, relatively isolated star formation will be used to illustrate the outstanding issues in massive star formation. The problem of initial conditions is particularly acute because there is a lack of observational evidence for regions capable of forming massive stars *before* star formation actually begins. By analogy with the Pre-Protostellar Cores (PPCs) studied for low-mass star formation, one might call such regions Pre-Proto-cluster Cores (PPcCs). We will conclude with some speculation about what such cores might look like and possibilities for their detection.

1. Introduction

Understanding the formation of massive stars is crucial to an understanding of the formation of stars in general and of galaxies. Many, perhaps most, stars form in clustered environments where massive stars are present (Lada 1992, Williams & McKee 1997). Only massive star formation is readily studied at the distances of other galaxies. In particular, the discovery that star formation at substantial redshifts is often heavily obscured by dust (e.g., Frayer et al. 2000; Chapman et al. 2001) indicates that study of the history of star formation in galaxies, hence the major part of galaxy formation, can be related to what we learn about massive star formation in our own and nearby galaxies.

Here we consider a number of issues surrounding the formation of massive stars, beginning with a comparison to what we know about the formation of low mass stars, proceeding through some systematic studies of early stages of massive star formation, and ending with some speculations about the initial conditions for massive star formation.

2. An Evolutionary Paradigm?

In the case of low mass stars, a well-established evolutionary paradigm prevails, and a standard model of star formation (Shu et al. 1987) provides a detailed target for observational tests. Various alternative models have also been proposed

and observers are beginning to compare these models to observations. The evolutionary paradigm is based on the class system (Lada & Wilking 1984, Lada 1987), originally proceeding from Class I (deeply embedded) to III (revealed star, weak-line T Tauri star) via Class II (roughly the same as classical T Tauri stars).

The recent advances in submillimeter capability have revealed a self-luminous phase that is still more embedded than Class I, and André, Ward-Thompson, & Barsony (1993) called this phase Class 0. The initial conditions for low mass star formation appear to be amenable to study in dense regions without any evidence for internal luminosity. Variously called Pre-Protostellar Cores (PPCs), pre-stellar cores, or Class -1 sources, these objects first became obvious as peaks of submillimeter emission. While they roughly coincide with molecular emission regions, the molecular line emission did not directly reveal the high densities, apparently because of substantial molecular depletion (e.g., Caselli et al. 2001), caused by the high densities and low temperatures in the cores of these regions. The temperatures are low enough ($T_D \sim 7$ K) that even the submillimeter emission is decreased toward the centers (Evans et al. 2001), but the dust continuum emission is much more revealing than the molecular line emission that has usually been used to trace dense regions.

The extended class system relies on a mixture of slopes (Lada & Wilking 1984, Lada 1987), peaks, and ratios (André et al. 1993) in the spectral energy distribution (SED) of dust emission. An alternative that unifies these methods and provides a continuous variable is the bolometric temperature (T_{bol}) introduced by Myers & Ladd (1993). Chen et al. (1995) showed that the class boundaries corresponded well to certain values of T_{bol} . However, T_{bol} , being defined by the spectrally averaged mean frequency, can be heavily affected by emission at relatively short wavelengths, where geometrical effects are conflated with evolutionary effects. For the early stages, there are two important boundaries: Class -1 to Class 0; and Class 0 to Class I. There are usually insufficient measurements to define T_{bol} for Class -1 sources; the test for Class -1 status is that there is no evidence for internal luminosity. For the Class 0/I boundary, one can use either $T_{bol} = 70$ K (Chen et al. 1995) or the ratio of emission beyond $350 \mu\text{m}$ to total luminosity, L_{submm}/L (André et al. 1993).

To what extent can we carry the observational paradigm and theoretical models for low-mass star formation over to the case of massive star formation? Working with a modest sample size (14), van der Tak et al (2000) found rather poor correlations between different potential tracers of age. It is not very surprising that the SED may not correlate with evolution in the same way as for low mass stars; for massive stars forming in clusters, the SED will be dominated by the most luminous object that is still embedded and the evolution of the various objects is unlikely to be highly synchronized. The Class II phase in particular may have little meaning: for low mass stars, this is the phase when the SED is dominated by a disk; the presence of disks around massive stars is less firmly established. Finally, the evolution of massive stars is so much faster that we cannot expect the gentle unfolding of the SED as the dust moves from envelope to disk to star in the low mass case. Instead, massive stars reach the main sequence, form HII regions, blow ionized winds, etc. before much of the material in the envelope has fallen in.

What other evolutionary tracers might prove useful? Clearly, the emergence of an HII region, first as an ultra-compact HII region, marks an important evolutionary boundary. If we are looking for the earliest stages, we want to study sources before UC HII regions form. There are two general ideas for evolutionary tracers at earlier times: masers and chemical signatures. While OH masers appear to be associated with HII regions, H₂O and possibly CH₃OH (e.g., Minier, Conway, & Booth 2001) masers appear to be associated with early stages, when molecular outflows produce shocks. Hot cores (warm, dense, chemically-rich regions) also appear to precede UC HII regions (see van der Tak 2002 for a discussion of this approach). The hot cores could in principal be heated internally (and hence analogous to Class 0 sources) or externally (hence analogous to Class -1 sources).

There have been many detailed studies of individual regions of massive star formation, but systematic studies of large samples of regions using uniform analytical methods are just becoming available (e.g., Plume et al. 1992, 1997, Bronfman et al. 1996, Sridharan et al. 2001). In the next section, we report on recent work on the sample identified by Plume et al. (1992).

3. Studies of Regions Associated with Water Masers

Water masers provide a large sample of objects with accurate positions for further study (e.g., Cesaroni et al. 1988). Many masers are *near* UC HII regions, but their positions do not coincide, consistent with the masers revealing an earlier stage. In addition, the presence of a H₂O maser ensures the existence of some very dense gas. The models of these masers also require shocks, suggesting that some star formation and associated outflow has begun. Consequently, we have pursued a series of studies of the gas and dust in the directions of water masers, beginning with a survey for emission in the $J = 7 \rightarrow 6$ transition of CS (Plume, Jaffe, & Evans 1992). A large fraction of the maser sources were detected in the CS $J = 7 \rightarrow 6$ survey, leading to a follow-up study using CS $J = 2 \rightarrow 1$, $J = 3 \rightarrow 2$, $J = 5 \rightarrow 4$, and in a few cases, $J = 10 \rightarrow 9$ transitions to constrain the density via LVG calculations of the molecular excitation (Plume et al. 1997). For many sources, C³⁴S data provided a check on optical depth effects in CS. That study found high densities in many sources, with a mean in the log of density, $n(\text{cm}^{-3})$, of $\langle \log n \rangle = 5.9$, with the average taken over 71 sources.

Plume et al. (1997) also mapped a few sources crudely (cross-scans) to estimate sizes and masses. To obtain better data on sizes, masses of dense gas, density distributions, etc., we have made fully sampled maps of a large fraction of the Plume et al. sample. We mapped 63 regions in CS $J = 5 \rightarrow 4$ (Shirley et al. 2002) and 24 regions in CS $J = 7 \rightarrow 6$ (Knez et al. 2002). In addition, we have mapped the 350 μm continuum emission from dust toward 51 of these regions (Mueller et al. 2002). Details of the observations and analysis can be found in those papers, and a more complete study of one of the objects can be found in Lee et al. (2002). Here we focus on the overall results, summarizing and comparing the results from the different tracers, while accounting for differences among the samples in the different studies.

For all the samples, the FWHM size of each core was determined by deconvolving the telescope main beam FWHM from the observed FWHM of the core. In most cases, the deconvolved angular sizes determined in this way were slightly larger than the beam size, characteristic of a power-law emission distribution (Terebey et al. 1993). Also, the CS $J = 7 \rightarrow 6$ sizes were smaller than the CS $J = 5 \rightarrow 4$ sizes, as expected for a centrally peaked density distribution because the critical density for the $J = 7 \rightarrow 6$ line is 3 times greater than that for the $J = 5 \rightarrow 4$ line (cf. Evans 1999). For power law distributions, the size defined in this way should not be considered a physical boundary. Instead, we use it, along with the distance, to calculate a fiducial radius for convenient comparisons.

Similarly, the mass in a power law distribution can only be specified for a given radius; when comparing masses from various techniques, it is important to compare for the same fiducial radius. Because the CS $J = 5 \rightarrow 4$ maps have the largest extents, thus tracing the core farther down the density distribution, we compare all masses calculated to be inside the radius of the CS emission: $r_{CS} = (D/2)\theta_s$, where θ_s is the FWHM angular extent of the map of CS $J = 5 \rightarrow 4$ emission and D is the distance.

3.1. Models

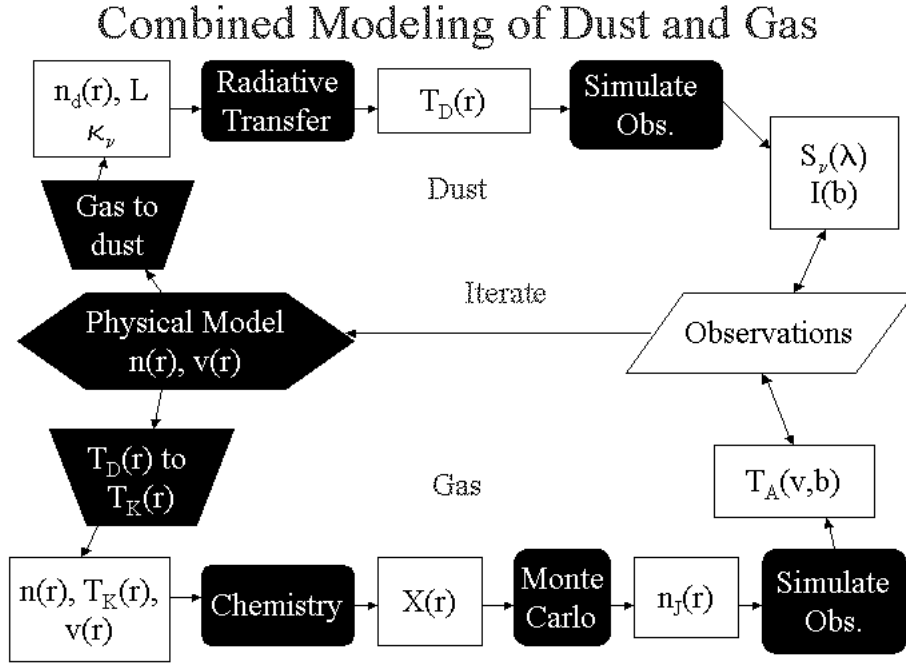


Figure 1. The modeling scheme is shown, with the modeling of dust emission following the top loop and the modeling of emission from gas following the bottom loop. Not all steps are fully implemented yet.

The modeling follows the scheme represented by Figure 1, though at present some of the processes are incompletely implemented. The modeling of the dust emission is described by Mueller et al. (2002). A density power law ($n(r) = n_0(r/r_0)^{-p}$) is assumed, a radiative transport code is used to compute a self-consistent $T_D(r)$, and the resulting $T_D(r)$ and $n(r)$ are used to compute the dust emission over the full SED. For comparison with maps of submillimeter continuum emission, the emission is convolved with the measured beam response and chopping is simulated. Comparison of the predicted intensity profile to that obtained in the observations allows one to choose the best fitting power law index for the density. Comparison to the observed integral of the SED constrains the internal luminosity of the forming stars, while comparison to the emission at submillimeter wavelengths constrains n_0 and hence the mass. The mass also depends on the assumed opacity at $350 \mu\text{m}$ ($\kappa_\nu(350)$), and the overall shape of the SED depends on the full behavior of the dust opacity as a function of frequency ($\kappa_\nu(\nu)$). We assume the dust opacities given in column 5 of Ossenkopf and Henning (1994), hereafter OH5, but divide by 100 so that are given per gram of total mass (gas plus dust). These opacities have fit the SEDs from both low-mass (Evans et al. 2001, Shirley et al. 2001) and high-mass (van der Tak et al. 2000) star formation regions. They are appropriate for grains that have coagulated at high density and accreted thin ice mantles. Different choices for opacities make little difference in the optimum p , but they do affect the mass because only the product $M\kappa_\nu(350)$ enters the equation for the dust emission.

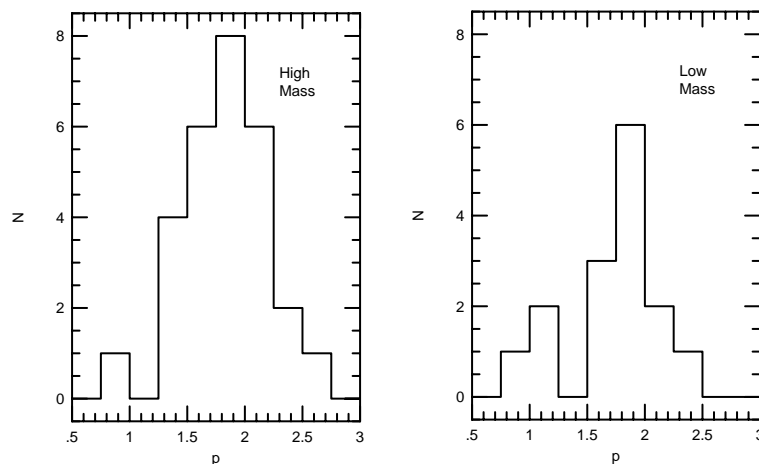


Figure 2. Histograms of p , best-fit density power law exponents for high-mass star forming regions on the left (Mueller et al. 2002) and for low-mass star forming regions on the right (Shirley et al. 2001, Young et al. 2001). All are based on modeling the radial distribution of the submillimeter continuum emission from dust.

For the 28 sources with models, Mueller et al. (2002) find a mean density index of $\langle p \rangle = 1.72 \pm 0.37$, with a distribution shown in Figure 2 (left panel). This value is considerably larger than that found by van der Tak et al. (2000), who modeled a subset of these sources. For that earlier work, the beam was

approximated as a Gaussian, while the observed beam, including azimuthally averaged sidelobes, was used in the models by Mueller et al. (2002). For sharply peaked intensity distributions, the details of the beam profile make a substantial difference; source-by-source comparison indicates that Mueller et al. find values of p larger than those found by van der Tak et al. by about 0.4 on average. The $\langle p \rangle$ found by Mueller et al. (2002) is consistent within the uncertainties with that found by Beuther et al. (2001) ($\langle p \rangle = 1.6 \pm 0.5$) for a differently-selected sample of regions forming massive stars. These power-law indices are also similar in the mean to those found for isolated cores forming low mass stars (Shirley et al. 2000, 2001; Young et al. 2001; Motte & André 2001). In Figure 2, right panel, we show the histogram for the combined sample of low-mass cores modeled by Shirley et al. (2001) and Young et al. (2001), for which $\langle p \rangle = 1.63 \pm 0.40$. While the means agree, the distributions may be different, though larger samples are still needed. The low-mass regions primarily have $p \sim 2$; the smaller peak between 1 and 1.5 is composed of sources that are quite aspherical. The distribution of p for regions forming massive stars appears to have a larger intrinsic spread.

The detailed modeling of the CS emission (Knez et al. 2002) is at an early stage, with only one source (M8E) modeled, and some of the processes in the bottom loop of Figure 1 are incompletely implemented. In particular, we use the $T_D(r)$ from the dust modeling and currently assume $T_K = T_D$ (a good assumption at the densities probed by CS emission). The turbulent velocity dispersion is assumed to be constant, and no systematic motions (e.g., collapse) are assumed. Instead of running a chemical model, we assume a constant CS abundance, which is adjusted to match the optically thin emission from $\text{C}^{34}\text{S } J = 5 \rightarrow 4$. Various values of p were used to allow a determination independent from that of the dust emission. For M8E, the CS prefers a slightly lower value of p than the dust: 1.6 rather than 1.75. Given the uncertainties and the assumptions, these are in quite good agreement.

3.2. Masses

Mueller et al. (2002) find a mean mass of gas and dust based on the dust emission within the FWHM of the $350 \mu\text{m}$ emission, $\langle M_D \rangle = 209 M_\odot$. Because the submillimeter emission has the smallest beam, and because the submillimeter sample does not include the more massive cores in the full sample, this mass is much less than the mean virial mass, $\langle M_V \rangle = 4550 M_\odot$, determined from the CS emission (Shirley et al. 2002). In addition, that estimate of virial mass assumed constant density and used the FWHM velocity width of the CS $J = 5 \rightarrow 4$ line, which is broadened by optical depth effects. We can correct the virial mass M_V for the density power law index, according to (Bertoldi & McKee 1992),

$$M_V = \frac{5(1 - \frac{2p}{5})r_{CS}\Delta v^2}{8\ln 2G(1 - \frac{p}{3})}$$

where the factor $8\ln 2$ comes from converting from mean square velocity to FWHM linewidth (Δv), and r_{CS} is the radius defined above for the CS $J = 5 \rightarrow 4$ emission. For this calculation, we use the FWHM of the C^{34}S line, which corrects for saturation broadening of the CS lines. Preliminary comparisons of ^{13}CS

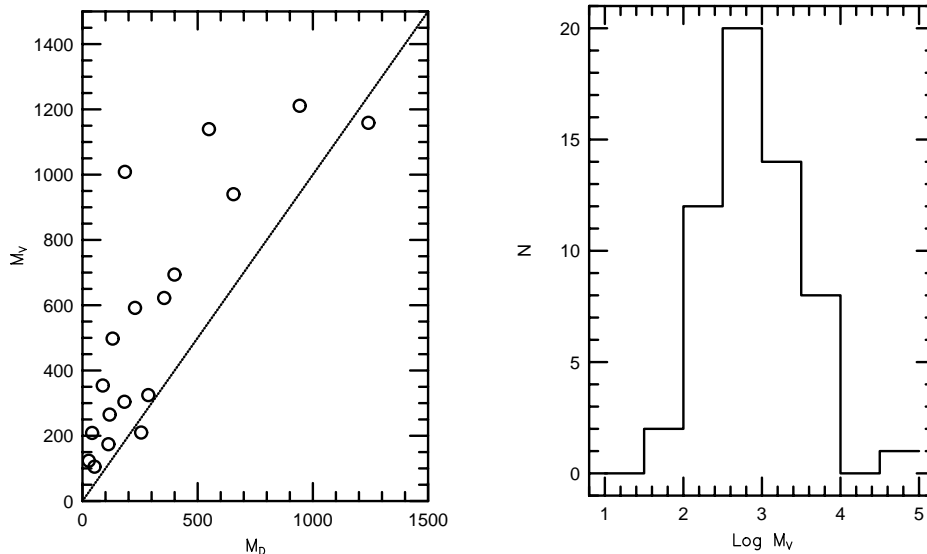


Figure 3. The corrected CS virial mass (density power law and linewidth broadening corrected) compared to the total (gas plus dust) mass based on models of the dust emission for 18 sources (left) and the corrected CS virial mass histogram for the entire sample of 57 sources (right).

and $C^{34}S$ spectra indicate that $C^{34}S$ $J = 5 \rightarrow 4$ linewidths are not broadened due to optical depth effects.

For comparison, we calculate the total mass based on the model of the dust emission, but integrated out to the same radius (r_{CS}) as used for the virial mass:

$$M_D = \frac{4\pi\mu m_H n_0}{r_0^{-p}} \int_0^{r_{CS}} r^{2-p} dr = \frac{4\pi\mu m_H n_0 r_{CS}^{3-p}}{(3-p)r_0^{-p}}$$

where μm_H is the mean molecular mass and n_0 is the density at r_0 . Because the value of n_0 is fixed by matching the observed flux density at $350 \mu\text{m}$, $n_0 \propto 1/\kappa_\nu(350)$. The ratio of the virial mass to the total (gas and dust) mass determined from the dust modeling then depends on measured and assumed quantities as follows:

$$M_V/M_D \propto \Delta v^2 r_{CS}^{p-2} / n_0 \propto \Delta v^2 \kappa_\nu(350) r_{CS}^{p-2}$$

For the 18 sources with all the required data and models, $\langle M_V/M_D \rangle = 2.4 \pm 1.4$ (see Figure 3). Because the opacities from different dust models vary by up to a factor of 10 (e.g., Ossenkopf & Henning 1994), this discrepancy is not very large. The agreement of the two very different mass estimates at this level suggests that both the assumptions underlying the virial mass estimate and the OH5 opacities at $350 \mu\text{m}$ are quite good. A factor of about 2 decrease in $\kappa_\nu(350)$ from the OH5 value would bring them into agreement on average.

Based on the good agreement of the masses on average, we calculated the virial masses for the rest of the sample, assuming the mean value of p and correcting for linewidth broadening in the CS $J = 5 \rightarrow 4$ line statistically (Shirley

et al. 2002). The resulting mass distribution has a mean value of $2030 \pm 620 M_{\odot}$. Recall that this number refers to the mass inside r_{CS} ; if the core extends to twice this radius with the same power law in density, the estimate of M_V grows by a factor of 2, while the mass from dust emission grows by 2^{3-p} or a factor of 2.4 for the mean p , leading to estimates of 4000 to 4900 M_{\odot} , for the mean mass. While the mass histogram appears peaked, selection effects against small sources are present at the mean distance of sources in this sample: 5.5 ± 3.7 kpc. For sources above 1000 M_{\odot} , the distribution could be fitted by a power law in mass with an exponent of 1.8 to 2.0 (Shirley et al. 2002).

3.3. Evolutionary Indicators

Evolutionary indicators (T_{bol} , L_{smm}/L_{bol} , and p) for the water maser sample and for low mass protostars observed with SCUBA at 850 and 450 μm (Young et al. 2001, Shirley et al. 2001, Evans et al. 2001, Shirley et al. 2000) are plotted in Figure 4. Based on the evolutionary scheme for low mass star formation, T_{bol} would be expected to increase while L_{smm}/L_{bol} would decrease as the envelope dissipates. Indeed, for low mass protostars, these trends seem to hold for a small sample of sources in the most embedded phases of evolution (PPC through Class I). The water maser sources weakly follow a similar trend; however, the water maser sample does not cover as wide a range in T_{bol} and L_{smm}/L_{bol} as the low mass core sample. Preliminary analysis of dust models for both high and low mass cores do not indicate a strong correlation of the density power law index, p , with T_{bol} . Both samples are biased towards more embedded regions and therefore sample a restricted range of T_{bol} and L_{smm}/L_{bol} . Each indicator has a different dependence of geometrical effects, such as outflow cavities, clumping, etc. T_{bol} and L_{smm}/L_{bol} are determined from the SED, while the density power law index, p , probes the density distribution in a different way. While larger samples covering a wider range of the evolutionary parameters are needed, it seems that the traditional evolutionary indicators for low mass star formation may have some utility for massive stars, at least at the early (Class 0 and I) stages.

3.4. Summary

The results so far from the study of water maser sources indicate that conditions in regions forming massive stars are quite different from those in regions forming low mass stars. The total mass of dense ($n \sim 10^6 \text{ cm}^{-3}$) gas is much greater, the turbulence is much higher for a given size, and, once stars have formed, the temperature is much higher. For the subset of sources with adequate data, the luminosity to mass ratio is $192 \pm 145 L_{\odot}/M_{\odot}$ for the mass of *dense* gas determined from the virial mass within r_{CS} . For the masses based on the dust emission, the same ratio is $334 \pm 231 L_{\odot}/M_{\odot}$. The latter number may be more relevant for comparison to observations of distant galaxies where long wavelength dust emission is used to trace mass. These numbers are for 18 sources that have models for the dust emission, and are still preliminary until more sources can be added.

These values for L/M are much higher than that inferred from CO studies, which provide masses for the whole molecular cloud. The average value from CO studies is $\langle L/M \rangle = 4 L_{\odot}/M_{\odot}$ (Mooney & Solomon 1988) and the distribution

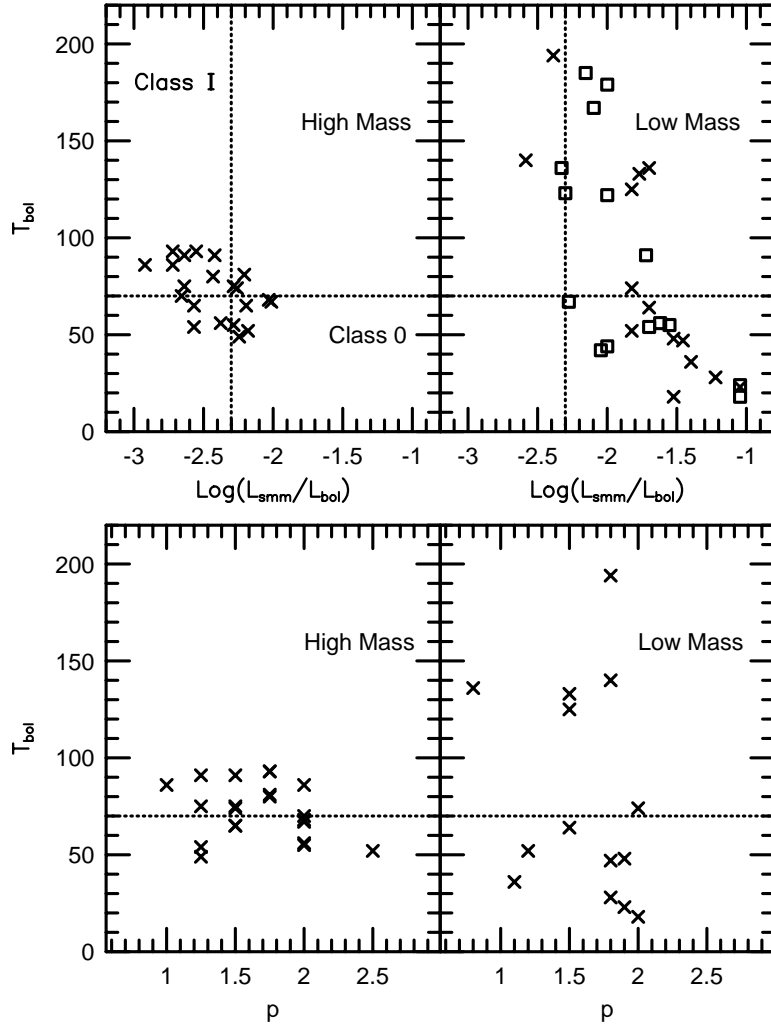


Figure 4. Potential evolutionary indicators for low and high mass star forming regions. The crosses indicate sources with models, while the open boxes in the upper right diagram represent sources that have not been modeled. The dashed lines indicate the boundary between Class 0 and Class I protostars in the low mass evolutionary scheme (Class 0 sources should have $T_{bol} < 70$ K and $L_{submm}/L_{bol} > 0.005$). Note that the two tracers (T_{bol} and L_{submm}/L_{bol}) disagree for a substantial number of the low mass cores, suggesting that the dividing lines may need revision.

spreads over a factor of 10^2 (Evans 1991). The dense gas provides a much better guide to the star formation rate and efficiency, consistent with the conclusions of Gao & Solomon (2000), who showed that HCN correlates much better than CO with star formation indicators in a large sample of galaxies. The L/M for dense gas is comparable to the values inferred for starburst galaxies, based on CO emission: $L/M \sim 100$ (Kennicutt 1998, Sanders et al. 1991). Starburst galaxies appear to form stars as if a large fraction of their molecular gas content behaves like the dense cores associated with water masers.

4. The Initial Conditions

So far, all the regions studied already have ongoing star formation. What initial conditions lead to the conditions in the observed regions? By analogy with the Pre-Protostellar Cores (PPCs) for low mass star formation, the initial conditions for massive, clustered star formation might be referred to as Pre-Proto-cluster Cores (PPclCs, an acronym chosen deliberately to avoid its future use). Based on the mean properties of the H₂O maser sample, we would expect the following properties. They would be dense ($n \sim 10^6 \text{ cm}^{-3}$) and massive ($M \sim 5000 M_{\odot}$). The linewidth is a question: if the turbulence is stirred up by star formation, it could be less before star formation begins; however, the virial linewidth for a core of the mean mass would be 7.5 km s^{-1} . Before an internal luminosity source develops, the PPclC should be very cold on the inside because it is heated only externally by the interstellar radiation field (ISRF). Studies of low-mass PPCs indicate T_D dropping to 7–8 K at the center (Evans et al. 2001, Zucconi et al. 2001).

So far, we have no clear examples of such objects! There are less massive candidates, but nothing we have found in the literature approaches these properties. Why do we lack examples? There are several possible explanations:

1. PPclCs will be very rare.
2. Appropriate searches have not been made.
3. PPclCs never exist.

The first explanation arises because massive star formation is rare in general and because PPclCs should evolve rapidly to form stars. The second explanation can certainly be part of the answer. The low mass PPCs were found only recently, using submillimeter continuum observations of starless cores originally identified by visual obscuration. While molecular line emission identified the general region, the high densities in the PPCs became apparent only with submillimeter dust emission studies. The molecular tracers fail to trace the densest regions of PPCs, apparently because of a combination of opacity and heavy depletion onto dust (e.g., Kramer et al. 1999, Caselli et al. 2001). Because no obvious signposts like maser emission mark the PPclCs, unbiased submillimeter surveys of large regions of distant molecular clouds are needed to find them. While such surveys are becoming possible and should be attempted, it is only fair to note the third explanation. Regions forming clusters may never go through a PPclC phase if lower-mass stars form while the full mass is being

assembled. In that case, one might see various signposts of lower mass star formation (outflows, infrared emission) associated with a *cluster* of cores that are merging to form the truly massive cores observed at later stages.

Some possible candidates for PPclCs may be found from large scale surveys. For example, Lada et al. (1991) surveyed 3.6 square degrees of the L1630 cloud in CS $J = 2 \rightarrow 1$ emission, finding numerous dense cores. The large cores all had ongoing star formation; follow-up studies (Lada et al. 1997) showed that the starless cores were all of modest mass ($M \sim 10M_{\odot}$). The most promising candidates at present are the mid-infrared-dark clouds found by the MSX mission that lack IRAS emission (Egan et al. 1998). Follow-up studies using H_2CO (Carey et al. 1998a) found massive ($M \sim 10^3 M_{\odot}$), cold ($T_D \sim 10$ K) cores with $n \sim 10^6 \text{ cm}^{-3}$. Maps of the submillimeter dust emission (Carey et al. 1998b) showed a string of cores, some of which harbor molecular outflows. The outflows indicate that some star formation may have begun, but these objects at least seem to be at a very early evolutionary stage.

4.1. A Model for the PPclC

To provide a target for possible searches, we have constructed a model of a PPclC based on the mean properties of the H_2O maser sample: $M = 4600M_{\odot}$, $p = 1.72$, and $d = 5.5$ kpc. The outer radius of the model was taken to be 0.76 pc, twice the mean radius from the CS maps. At the mean distance of 5.5 kpc, this radius translates to $\theta_s = 56''$. The dust temperature was assumed constant at 10 K; while models of PPCs indicate lower T_D in the center, PPclCs may exist in regions of higher radiation fields. OH5 opacities were assumed. Observations of the model with various past, current, and future instruments were simulated. The results are shown in Figure 5. The solid line is the total emission, while the circles show the emission into the beam of the instrument. The horizontal bars show the limits for 1 sec of integration. It is not surprising that IRAS did not detect these objects; SIRTf could detect them at $160 \mu\text{m}$, but that channel will be saturated for most regions of molecular gas just from the extended cloud emission. The best regime in which to search for such objects is the millimeter to submillimeter, and systems with fairly large beams and fields of view are ideal for the large-scale blind surveys that will be needed. A good example of such an instrument is Bolocam, operating on the CSO (Glenn et al. 1998).

5. Summary

The formation of massive stars occurs in parts of molecular clouds that are much denser and more turbulent than the bulk of the molecular gas. Compared to the regions forming low mass stars, the birthplaces of massive stars have high densities over much larger regions and their linewidths are much greater than those inferred from the linewidth-size relation. A clear evolutionary sequence is difficult to establish, but regions surrounding water masers should be younger than those around ultra-compact HII regions. Studies based on H_2O masers find a distribution of masses of dense ($n \sim 10^6$) gas that extends to quite large masses. While affected by selection biases, a mean value of 2000–4000 M_{\odot} is found, enough to form large clusters of stars. Modeling the radial profiles of submillimeter emission from dust indicates that power laws in density ($n(r) \sim$

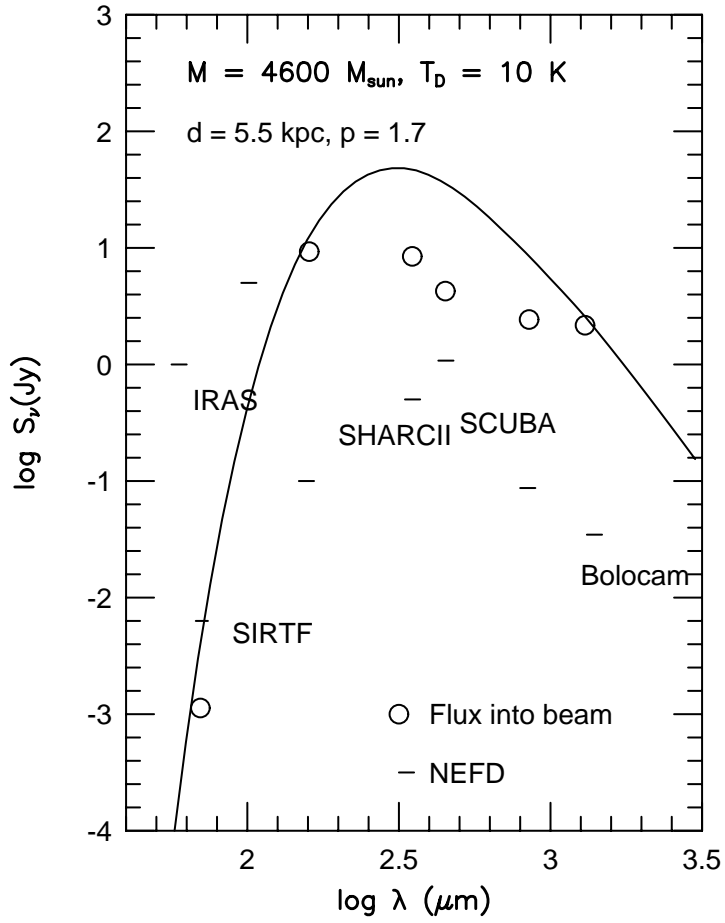


Figure 5. The SED of a putative Pre-Proto-cluster Core, based on typical properties of the cores found around water masers, but assuming a constant dust temperature of 10 K. The emission from the overall core is shown by the solid line, while the flux density contained within a single beam of various instruments is shown as open circles. The horizontal bars show the NEFD of these instruments.

r^{-p}) fit the data with a mean $p = 1.72$, rather similar to that found for molecular cores around ultra-compact HII regions (Beuther et al. 2001) and to low mass star-forming cores (Shirley et al. 2001; Young et al. 2001).

Acknowledgments. This work has been supported by NASA grants NAG5-7203 and NAG5-10488, by NSF grant AST-9988230, and by the State of Texas.

References

- André, P., Ward-Thompson, D., & Barsony, M. 1993, ApJ, 406, 122
- Bertoldi, F., & McKee, C. 1992, ApJ, 395, 140
- Beuther, H., Schilke, P., Menten, K. M., Motte, F., Sridharan, T. K., & Wyrowski, R. 2001, ApJ, in press (astro-ph/0110370)
- Bronfman, L. Nyman, L.-A., May, J. 1996, A&AS, 115, 81
- Carey, S. J., Clark, F. O., Egan, M. P., Price, S. D., Shipman, R. F., & Kuchar, T. A. 1998a, ApJ, 508, 721
- Carey, S. J., Redman, R. O., Feldman, P. A., Egan, M. P., & Shipman, R. F. 1998b, American Astronomical Society Meeting, 193, 6525
- Caselli, P., Walmsley, C. M., Zucconi, A., Tafalla, M., Dore, L., & Myers, P. C. 2001, ApJ, in press (astro-ph/109023)
- Cesaroni, R., Palagi, R., Felli, M., Catarzi, M., Comoretto, G., DiFranco, S., Giovanardi, C., & Palla, F. 1988, A&AS, 76, 445
- Chapman, S. C., Richards, E. A., Lewis, G. F., Wilson, G., & Barger, A. J. 2001, ApJ, 548, L147
- Chen, H., Myers, P. C., Ladd, E. F., & Wood, D. O. S. 1995, ApJ, 445, 377
- Egan M. P., Shipman, R. F., Price, S. D., Carey, S. J., Clark, F. O., & Cohen, M. 1998, ApJ, 494, L199
- Evans, N. J., II 1991, in *Frontiers of Stellar Evolution*, ed. D. L. Lambert, (San Francisco:Astron. Soc. Pacific), 45
- Evans, N. J., II 1999, ARA&A, 37, 311
- Evans, N. J., II, Rawlings, J. M. C., Shirley, Y. L., & Mundy, L. G. 2001, ApJ, 557, 193
- Frayser, D. T., Smail, I., Ivison, R. J., & Scoville, N. Z. 2000, AJ, 120, 1668
- Gao, Y. & Solomon, P. 2000, American Astronomical Society Meeting, 197, 9603
- Glenn, J. et al. 1998, SPIE, 3357, 326
- Kennicutt, R. C., Jr. 1998, ARA&A, 36, 189
- Knez, C., Shirley, Y. L., Evans, N. J., II, & Mueller, K. E., 2002, these proceedings
- Kramer, C., Alves, J., Lada, C. J., Lada, E. A., Sievers, A., Ungerechts, H., & Walmsley, C. M. 1999, A&A, 342, 257
- Lada, C. J. 1987, in *Star Forming Regions*, IAU Symp. 115, ed. M. Peimbert & J. Jugaku (Dordrecht: Reidel), 1
- Lada, C. J., & Wilking, B. A. 1984, ApJ, 287, 610
- Lada, E. A. 1992, ApJ, 393, L25

- Lada, E. A., Bally, J., & Stark, A. A. 1991, *ApJ*, 368, 432
- Lada, E. A., Evans, N. J., II, & Falgarone, E. 1997, *ApJ*, 488, 286
- Lee, J.-E., Young, C. H., Shirley, Y. L., Mueller, K. E., & Evans, N. J., II 2002, these proceedings
- Minier, V., Conway, J. E., & Booth, R. S. 2001 *A&A*, 369, 278
- Mooney, T. J., Solomon, P. M. 1988, *ApJ*, 334, L51
- Motte, F., & André, P. 2001, *A&A*, 365, 440
- Mueller, K. E., Shirley, Y. L., Evans, N. J., II, & Jacobson, H. R. 2002, these proceedings
- Myers, P. C., & Ladd, E. F. 1993, *ApJ*, 413, L47
- Ossenkopf, V., & Henning, Th. 1994, *A&A*, 291, 943
- Plume R., Jaffe, D. T., Evans, N. J., II 1992, *ApJS*, 78, 505
- Plume R., Jaffe, D. T., Evans, N. J., II Martin-Pintado, J., & Gómez-González, J. 1997, *ApJ*, 476, 730
- Sanders, D. B., Scoville, N. Z., & Soifer, B. T. 1991, *ApJ*, 370, 158
- Shirley, Y. L., Evans, N. J., II, Mueller, K. E., Knez, C., & Jaffe, D. T. 2002, these proceedings
- Shirley, Y. L., Evans, N. J., II, & Rawlings J. M. C., & Gregersen, E. M. 2000, *ApJS*, 131, 249
- Shirley, Y. L., Evans, N. J., II, & Rawlings J. M. C. 2001, in prep.
- Shu, F. H., Adams, F. C., & Lizano, S. 1987, *ARA&A*, 25, 23
- Sridharan, T. K., Beuther, H., Schilke, P., Menten, K. M., & Wyrowski, F. 2001, *ApJ*, in press
- Terebey, S., Chandler, C. J., & André, P. 1993, *ApJ*, 414, 759
- van der Tak, F. F. S. 2002, these proceedings
- van der Tak, F. F. S., van Dishoeck, E. F., Evans, N. J., II, & Blake, G. A. 2000, *ApJ*, 537, 283
- Williams, J. P., & McKee, C. F. 1997, *ApJ*, 476, 166
- Young, C. H., Shirley, Y. L., Evans, N. J., II, & Rawlings, J. M. C. 2001, in prep.
- Zucconi, A., Walmsley, C. M., & Galli, D. 2001, *A&A*, 376, 650